II MICROWAVE PHYSICS

A MICROWAVE SPECTROSCOPY

1 Microwave-Frequency Bridge

Staff M W P Strandberg
J G Ingersoll

Methyl fluoroform has been examined in the 5-mm bridge Since this molecule is a symmetrical top the study of its spectrum will be of interest For instance Stark effect measurements and contrifugal splitting of the levels will yield valuable data The molecule is too complex to make inter-atomic distance measurements feasible

2 Sweep Spectroscope

Staff M W P Strandberg
R Hillger
T Wentink
R L Kyhl Laboratory for Insulation Research

This system has been changed slightly with the addition of about 3 meters of "Stark guide", and an additional search method similar to that described by Hughes and Wilson[1] is in use A number of molecule have been given a cursory examination with little results

The system at present is being used to complete the inter-atomic measurements on carbon oxy-sulfide These measurements will include the series from the S=1 to S=2 transition to the S=4 to S=5 transition with C^{12} C^{13} S^{33} S^{34} and O^{16} as the constituent atoms

3 Audio-Frequency Bridge

Staff C I Beard

To compensate for the dielectric constant of the gas when measuring intensities with the audio-frequency bridge resort to the double-gas method has been found necessary R-f power is tapped from the ends of the two r-f bridge arms and fed through a magic T to a crystal detector as an r-f phase indicator This indicator enables the dielectric constant of the non-absorbing gas to be made equal to that of the absorbing gas

The major portion of time has been spent with Dr B P Dailey of Harvard analyzing the spectrum of methyl isothiocyanate a report of which will be made later

4 Caesium Spectrum

Staff Professor A G Hill
M W P Strandberg

Work progresses slowly Caesium has been contained satisfactorily in a quartz-lined cavity but work on other types of cavities continues

---

1 R A Hughes and E B Wilson, Jr Phys Rev 71, 562 (1947)

II B MOLECULAR BEAM RESEARCH

1 Hyperfine Structure of Hydrogen

Professor J R Zacharias
Dr B T Feld
L Davis, Jr
F S Julian
D E Nagle

Summary Radio-frequency transitions in atomic hydrogen are under study with the molecular beam magnetic resonance apparatus A tentative value of 1420 5 Mc has been obtained for the nuclear hyperfine splitting in the ground state of atomic hydrogen H^1 This result is higher than that predicted by the formula of Bethe[1], namely 1416 90 but recent results from the Columbia University laboratory[2] give an experimental value in essential agreement with the above

Theoretical Considerations In the absence of external fields the ground state of the hydrogen atom is split into two levels separated in energy by $h\Delta\nu$ and characterized by values of the total angular momentum quantum number $F = 1$ and $F = 0$, respectively The energy difference is due to the interaction of the proton magnetic moment with the magnetic field due to the atomic electron Electric quadrupole effects are absent because of the spherical symmetry of the nucleus

In a weak external magnetic field B the energy states are split and five radio-frequency lines are possible The energy levels are tabulated in Table I and plotted in Fig 1, the transition frequencies are listed in Table II and plotted in Fig 2 In these

TABLE I Energy Levels

F	m_F	$\frac{W_{F,m_F}}{h}$
1	1	$-\frac{1}{4}+\frac{1+x}{2}+x\frac{\varepsilon_1}{\varepsilon_J-\varepsilon_1}$
1	0	$-\frac{1}{4}+\frac{(1+x^2)^{\frac{1}{2}}}{2}$
1	-1	$-\frac{1}{4}+\frac{1-x}{2}-x\frac{\varepsilon_1}{\varepsilon_J-\varepsilon_1}$
0	0	$-\frac{1}{4}-\frac{(1+x^2)^{\frac{1}{2}}}{2}$

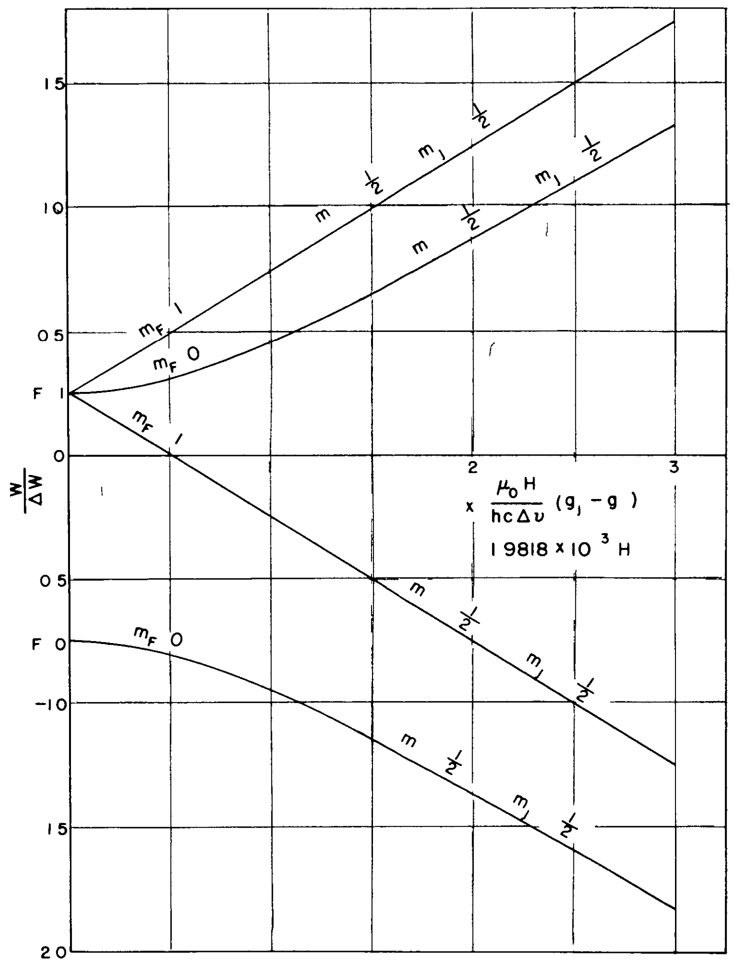

Figure 1 Energy levels of atomic hydrogen H^1 ground state $^2S_{\frac{1}{2}}$

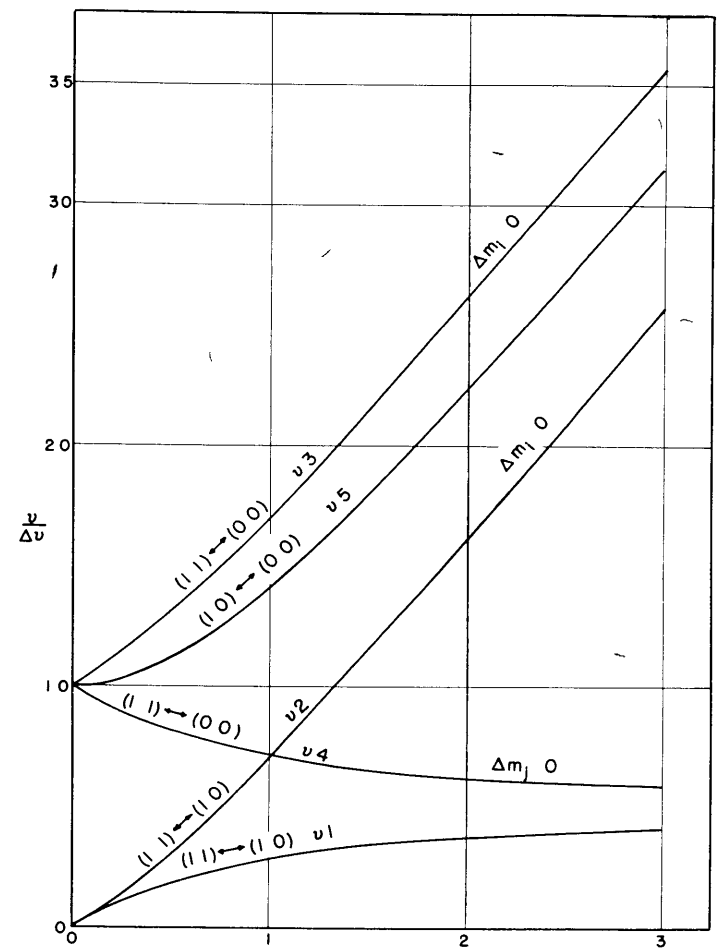

Figure 2 Transition frequencies

TABLE II Transition Frequencies

F, m_F	$F', m_{F'}$	$\nu/\Delta\nu$	
1,1	1,0	$\nu_1 = \frac{1 + x - (1 + x^2)^{\frac{1}{2}}}{2} + x \frac{g_1}{g_J - g_1}$	$\Delta F = \pm 1$ or 0, $\Delta m_F = \pm 1$
1 0	1,-1	$\nu_2 = \frac{-1 + x + (1 + x^2)^{\frac{1}{2}}}{2} + x \frac{g_1}{g_J - g_1}$	
1,+1	0,0	$\nu_3 = \frac{1 + x + (1 + x^2)^{\frac{1}{2}}}{2} + x \frac{g_1}{g_J - g_1}$	
1,-1	0,0	$\nu_4 = \frac{1 - x + (1 + x^2)^{\frac{1}{2}}}{2} - x \frac{g_1}{g_J - g_1}$	
1,0	0,0	$\nu_5 = (1 + x^2)^{\frac{1}{2}}$	$\Delta m_F = 0$, $\Delta F = 1$

expressions x is a dimensionless parameter which measures the strength of the perturbation by the field B

$$x = \frac{(g_J - g_1)\mu_0 B}{h\Delta\nu}$$

where g_J and g_1 are the negative gyromagnetic ratios of the electron and the proton, respectively h is Planck's constant and μ_0 is the Bohr magneton

In the molecular beam magnetic resonance method, atoms pass through a region of homogeneous field B wherein transitions are stimulated by an additional small magnetic field which oscillates with the frequency ν Inhomogeneous magnetic fields placed before and after the homogeneous field are adjusted so that hydrogen atoms normally miss the detector and the change in the magnetic moment of the atoms due to a transition in the homogeneous field is such as to cause focussing of the atoms onto the detector Under these conditions a rise in beam intensity may be expected when the frequency of the oscillating field is equal to the transition frequency ν[1]

Of these five lines the (1,0)⟷(0,0) is excited by a component of oscillating field parallel to the homogeneous field, a component which is very small in the present experiments This line probably could not be expected to be seen under present conditions

---

1 J M B Kellogg I I Rabi J R Zacharias Phys Rev 50 472 (1936)

The $(1,1)\leftrightarrow(1,0)$ and $(1,-1)\leftrightarrow(0,0)$ lines correspond to changes in magnetic moment unfavorable for refocussing and probably cannot be observed under present conditions Accordingly the two lines which were observed may be identified as the $(1\ 0)\leftrightarrow(1\ -1)$ and $(1,1)\leftrightarrow(0,0)$ transitions These are expected to have a constant frequency difference $\Delta\nu$

Description of Apparatus The apparatus has been described in some detail in the Progress Reports of October 15, 1946 and January 15, 1947 It consists essentially of (see Fig 3) an arc source of hydrogen suitable defining slits a magnet producing a field with uniform gradient perpendicular to the beam an r-f loop together with a magnet producing a uniform field perpendicular to the beam a third magnet similar to the first, an obstacle wire to remove the undeflected beam, and finally a detector of the Stern-Pirani type Excellent descriptions of similar apparatus have been given by Rabi Kellogg, and Zacharias[1,2] and by Zacharias[3] In the present apparatus the beam height is 3 cm and the widths of the various slits are

source slit	0025 cm	collimator slit	0025
obstacle wire	0038 cm	detector slit	0025

Approximate distances from the source slit are

collimator	21 3 cm
obstacle	58 6 cm
detector	72 cm

The present r-f wires are 2 cm long and the homogenous field 8 9 cm long

Method The currents in the deflecting magnets are set to values calculated from the geometry The r-f oscillator is set at some low frequency and the current through the magnet producing the homogeneous field is varied over a small region about the calculated value until a resonance appears in the form of increased detector current That negligible coupling exists between the r-f oscillator and the detector is verified by turning the beam off momentarily by means of a small shutter near the source A resonance curve is obtained holding the magnet currents constant and observing the magnitude of the refocussed beam as correlated with the oscillator frequency

Up to the present oscillator currents have been used which broaden the resonance beyond its natural width Sharpening the resonance probably requires a field more uniform than the present one

---

1 J M B Kellogg I I Rabi, and J R Zacharias Phys Rev 50 472 (1936)

2 I I Rabi J M B Kellogg and J R Zacharias Phys Rev 46 157 163 (1934)

3 J R Zacharias Phys Rev 61 270 (1942)

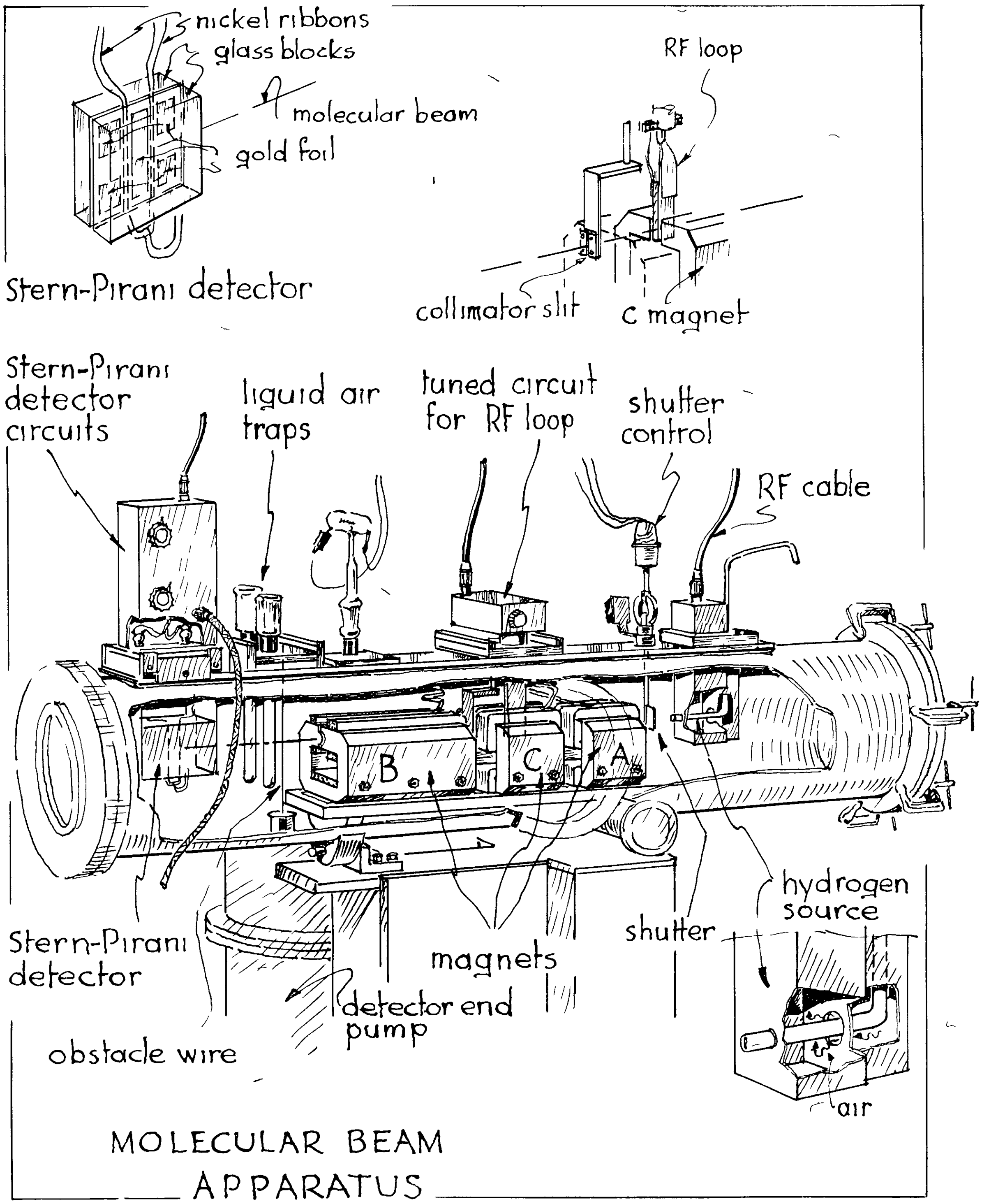
nickel ribbons
glass blocks
molecular beam
gold foil
Stern-Pirani detector
RF loop
collimator slit
C magnet
Stern-Pirani detector circuits
liquid air traps
tuned circuit for RF loop
shutter control
RF cable
A
B
C
hydrogen source
shutter
magnets
Stern-Pirani detector
detector end pump
obstacle wire
air
MOLECULAR BEAM APPARATUS

Figure 3

Results The following values for two lines have been observed

1,-1⟷1,0	1,1⟷0,0	$\Delta\nu$
30 00	1450 7	1420 7
56 22	1476 30	1420 08
62 75	1483 6	1420 85
62 89	1483 11	1420 22
62 95	1483 66	1420 71
83 60	1504 02	1420.42
		1420 5 ± 4

The width of the resonance curve at one-half maximum is of the order of 0 5 Mc (see Fig 4) It should be possible to narrow this to 0 05 Mc with the present apparatus

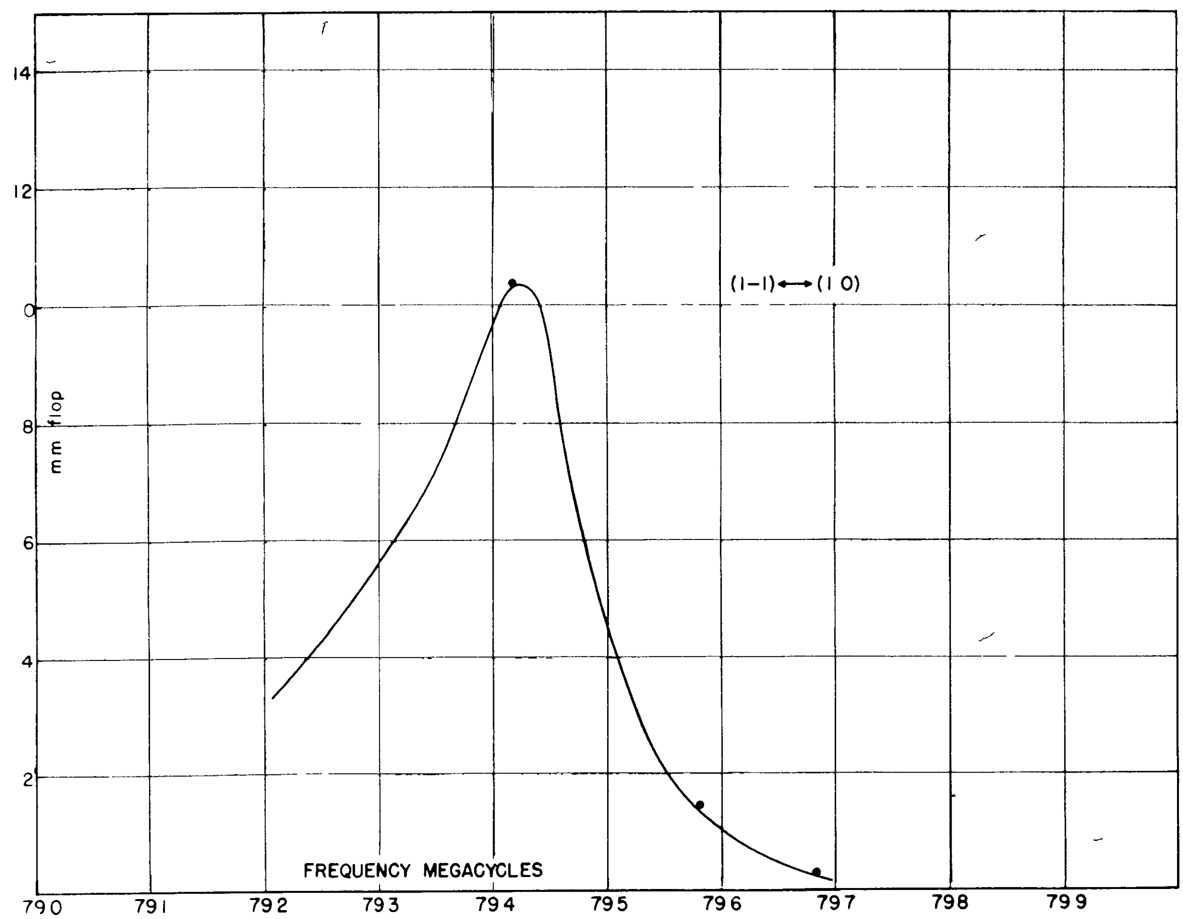

Figure 4 Resonance curve for the transition (1,-1)⟷(1,0) of hydrogen, H^1

2 Second Molecular Beam Resonance Apparatus

Staff Professor J R Zacharias
Dr B T Feld
C W Zabel

The second molecular beam resonance apparatus which was discussed in the Progress Reports of June 3, 1946 and April 15, 1947 has been designed and is under construction The magnet frame of one magnet for one inhomogeneous field has been completed and the second is being machined The magnets, source, and detector will be contained in two bronze castings 12 in in diameter and 5 ft long which will be bolted together to form a 10-ft tube The castings were successfully poured and are now being machined Before being assembled, each casting will be dipped in a tin bath to eliminate the danger of porous sections The final machining of critical surfaces will then be done on a 12-ft planing machine

Fore pumps diffusion pumps, and vacuum gages, and gage circuits are on hand so that work on the vacuum system can be started as soon as the machining has been completed

C LOW PRESSURE GAS DISCHARGES

Staff Professor S C Brown
Professor W P Allis
M A Biondi
E Everhart
M A Herlin
Donald E Kerr

Successful operation of a gamma-ray counter making use of a 3000-Mc gas discharge has been achieved Since the breakdown of a discharge in gases at these high frequencies does not depend upon secondary effects, and since the discharge is not controlled by positive ions shorter breakdown times and shorter resolving times are realized The normal operation of these discharges shows ambipolar diffusion as the controlling factor in loss of electrons, and a d-c sweeping field must be superimposed on the a-c power to eliminate electrons as rapidly as possible A quenching agent must be present to suppress secondary electron emission from positive ion bombardment of the walls.

The block diagram shows, schematically, the necessary circuits

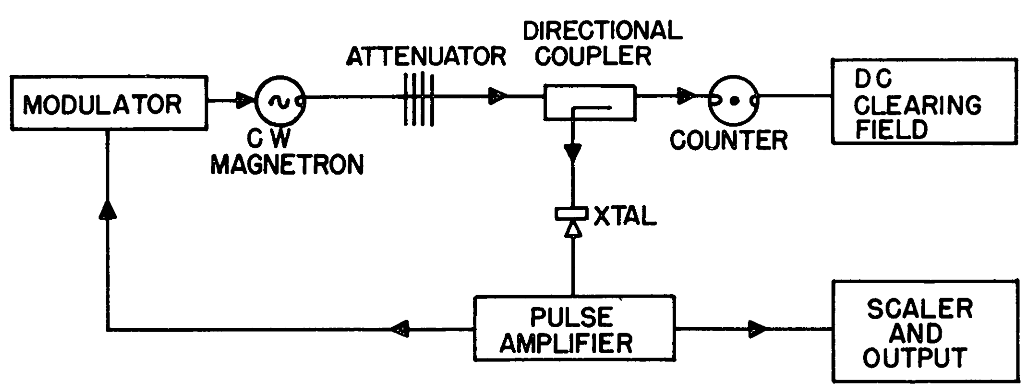

Figure 1 Block diagram

A 3000-Mc c-w magnetron feeds power to the counter which consists of a special coaxial mode cavity resonator described below When an ionizing particle enters the counter a discharge is initiated which mismatches the r-f line termination A directional coupler oriented to see this power change from the counter is connected through a crystal rectifier to a pulse amplifier This amplifier serves two functions, it pulses the magnetron modulator down so that the discharge in the counter terminates, and it feeds pulses to a scaler and message register serving as an indicator of the intensity of the ionizing radiation

A sketch of a preliminary type of counter resonant cavity is illustrated The cavity operates in a coaxial mode, the discharge taking place only in the center section of

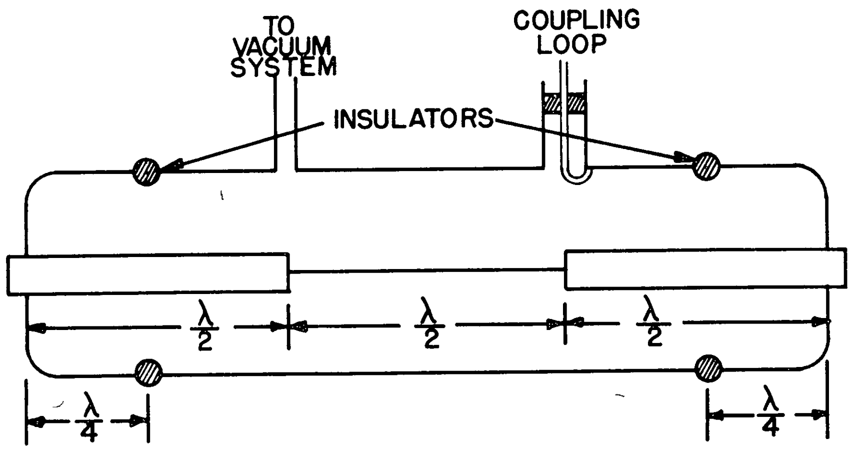

Figure 2 Sketch of u h f counter

the tube around a 10-mil coaxial conductor Discontinuities in the center coaxial member coincide with null planes in the electric field while the insulating rings for the d-c potential are constructed at zero current positions The center member is made of copper, while the shell is of copper-plated Kovar The cavity has a loaded Q of 360

In operation the power characteristics are somewhat similar to those found with a Geiger-Muller counter A typical run is shown in the following figure The sensitivity is the same as that of a Geiger-Muller counter of similar geometry The measured minimum resolving time is 25 μsec The speed of breakdown can be indicated by the measured rise time of the 3-volt output pulse This is slightly less than 10^{-8} seconds (see Fig 3)

A start has been made on the theory for breakdowns of the counter described above The problem is to determine the effect of the d-c clearing field on the a-c voltage at which breakdown occurs The next step involves a study of the time constants of the process Experimentally it is an advantage to be able to vary the d-c and the a-c fields independertly as they enter in the equations in a different way

Previous experiments of steady-state microwave gas discharges in cavities have measured operating voltages as a function of current and pressure These experiments are now being extended to include a measurement of breakdown voltage as well The breakdown voltage is controlled by electron diffusion in the gas A simple theory suggests that it can be predicted by a straight-forward boundary value solution in which the breakdown voltage appears Experiment will be compared with this theory The experiment above is

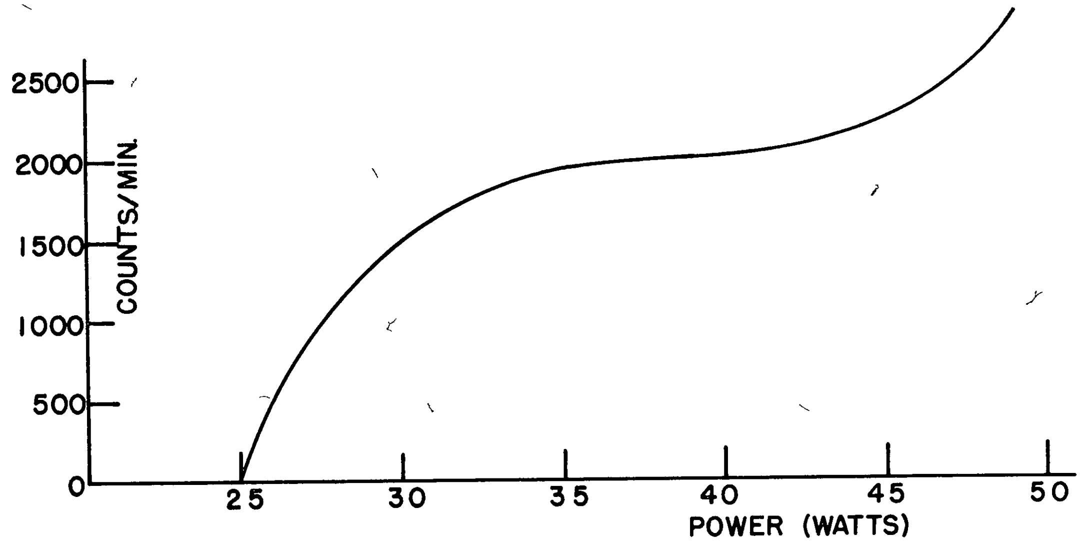

Figure 3 Plateau characteristics of u h f counter The above characteristics were measured with a counter filled with helium at 5 cm pressure and alcohol vapor at 1 cm pressure with a d-c sweeping potential of 500 volts

facilitated by a changed technique whereby one measures power from a calibrated probe attached to the cavity The cavity voltage is simply related to this power

The coaxial gas discharge cavity previously described[1] has been altered in the following way the glow discharge is now formed in the interior of the hollow center conductor between a fine center wire and the conductor The center conductor is perforated so that electrons formed by the glow discharge can be drawn into the region between the inner and outer conductors of the coaxial line In this region they can be accelerated by a potential on the outer conductor Essentially the microwave input impedance of the coaxial line is measured and related to the complex dielectric constant of the region between the inner and outer conductors It is believed that very high electron densities can be obtained Various ionization coefficients will be studied

The experimental results for the ambipolar diffusion experiment and for the experiment measuring operating characteristics of microwave discharges both show an anomoly which suggests that the frequency shift of a cavity may not be a linear function of the electron density within the cavity A possible explanation is that the electrons are not free as has been hitherto assumed but are partially bound to the positive ions particularly at high densities The following experiment is an attempt to find this effect under controlled conditions A coaxial half-wave cavity is made with its inner conductor perforated as in Fig 4 Inside the inner conductor a glow discharge as before furnishes electrons and ions The characteristics of the cavity Q and resonant wavelength can be measured We hope to be able to vary the electron density and positive ion densities independently

The experiments measuring ambipolar diffusion and other transient effects are being repeated with considerable effort to obtain very pure gases

The experiments of this group have hitherto been made using 10-cm microwaves

1 RLE Quarterly Progress Report January 15 1947 p 41

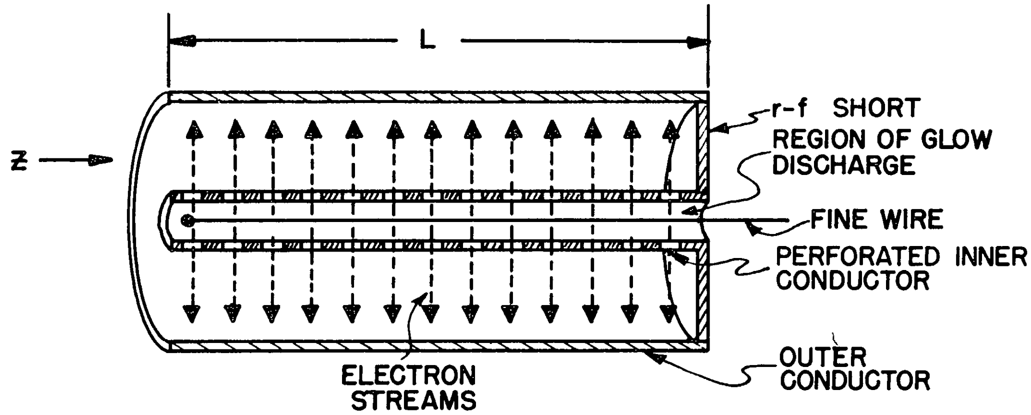

Figure 4 Coaxial di charge construction

Use of certain scaling principles should allow the predictions of phenomena at other wavelengths In order to make an experimental check on the scaling princip es, an experiment previously done at 10 cm has been repeated at 3 cm A glass bulb filled with helium was inserted in a 3-cm cylindr cal cavity Power from a 3-cm klystron was used to break down the helium The electric field strength across the discharge was measured and found nearly independent of input power A plot was made of field strength vs the pressure of the helium and compared with similar plots previously made from a duplicate experiment at 10 cm Agreement was qualitatively very good, but quantitatively differed from predicted results by 30 or 40 per cent Another check is being made of calibrations of various pieces of equipment to determine if the discrepancy is real

D LOW TEMPERATURE RESEARCH

1 <u>Helium Liquefiers</u>

Staff R P Cavileer

The first Collins Helium Cryostat made by the A D Little Co for M I T has run a total of 26 times since April 1 with but one failure

Since this cryostat was put into operation six months ago there have been only three performance failures and all of these have been due to the fact that the lubrication creeps from the stuffing boxes down the valve rods to a point where it freezes and siezes the rods

Various types of runs have been made, some to intermediate temperatures others for the purpose of liquefying hydrogen in the auxiliary liquefying coil and still others for making liquid helium In the 25 successful runs since April 1, there have been 133 hours of running time

The second Collins Helium Cryostat received from the A D Little Co has been set in place and is undergoing tests preliminary to operation

II D 2 Studies on Liquid Helium

Staff Professor C F Squire
J R Pellam

See "Ultrasonics" Section III B

3 Studies on Beryllium

Staff Professor C F Squire

In the last progress report, the resistivity of Be as a function of temperature was given and the unusually high residual resistivity at very low temperatures was emphasized In collaboration with Professor B E Warren and Dr J Fitzwilliam the X-ray structure has been investigated on the same specimen of Be The hexagonal, close packed structure was confirmed but in addition there were extra lines which demonstrated the presence of another structure A quantitative chemical analysis was then performed and the impurities turned out to be a total of 0 8 per cent, they were roughly:(Al = 0 4 per cent Fe = 0 1 per cent, Ca Cd, Si Sn Pb, Mg Mn Zn added up to the remainder of the impurities) It seems most likely that the X-ray lines which were not part of the regular hexagonal structure could be attributed to an alloy of Be with the 0 8 per cent impurity Such an alloy might have 9 Be atoms per atom of impurity It would seem most necessary to improve the purity of the Be specimen before making further physical measurements or before taking too seriously the lack of agreement between theory and experiment in such respects as specific heat paramagnetism, resistivity, etc We wish to acknowledge the assistance of Professor Albert Kaufmann Department of Metallurgy, M I T for the specimens of Be and for their analyses

4 Superconductivity at 1.25 cm

Staff Professor J C Slater
J B Garrison
E Maxwell

Since the last quarterly report further measurements have been made at 1 25 cms on both Hilger lead and less pure lead The results differ from those previously reported in that the resistivity in going from 7 5^{o} to 4 2^{o}K is now found to decrease by a factor of approximately 1600 and from 4 2^{o}K to 2^{o}K by a factor of about $2\frac{1}{2}$, these factors are found to be approximately the same for the pure and the impure lead The difference between these results and those previously reported is presumably due to improved techniques in preparing the samples and possibly also to the higher vacuum ($\sim 10^{-5}$ mm Hg at room temperature) now obtained inside the cavities Current results indicate that the rate of change of resistance with temperature is zero at 2^{o}K, which is the lowest temperature attainable at present It is not known whether the resistance at 2^{o}K represents the true residual resistance of the sample or whether it is due to surface conditions

Measurements made in the temperature range from room temperature to 8^{o}K seem to indicate that the r-f resistance decreases less rapidly than the d-c resistance More accurate d-c measurements are in progress using samples of lead wire extruded from the same stock from which the cavities are made

It is now felt that the measuring equipment and techniques are adequate to obtain relative Q values over the entire temperature range from room temperature to 2°K to better than 10 per cent accuracy Since accurate absolute Q measurements can easily be made at room temperature it is expected that in the near future absolute r-f resistivity data will be obtained for comparison with theory

As a check on the methods thus far used it is planned to make ringing-time measurements in the near future Since such measurements give the absolute value of the loaded Q of the cavity and since the methods thus far used give the ratio of the unloaded Q to the window Q the combination gives the absolute value of the unloaded Q without reference to room temperature measurements

It is also planned to make measurements on pure tin Tin has a transition temperature of 3 7°K and it will therefore be possible to obtain the exact shape of the resistance vs temperature curve since accurate temperature control can be achieved in the region from 4 2° to 2°K by immersion in liquid helium

Figure 1 shows a typical set of data ρ = resistivity at T°K ρ_0 = resistivity at room temperature

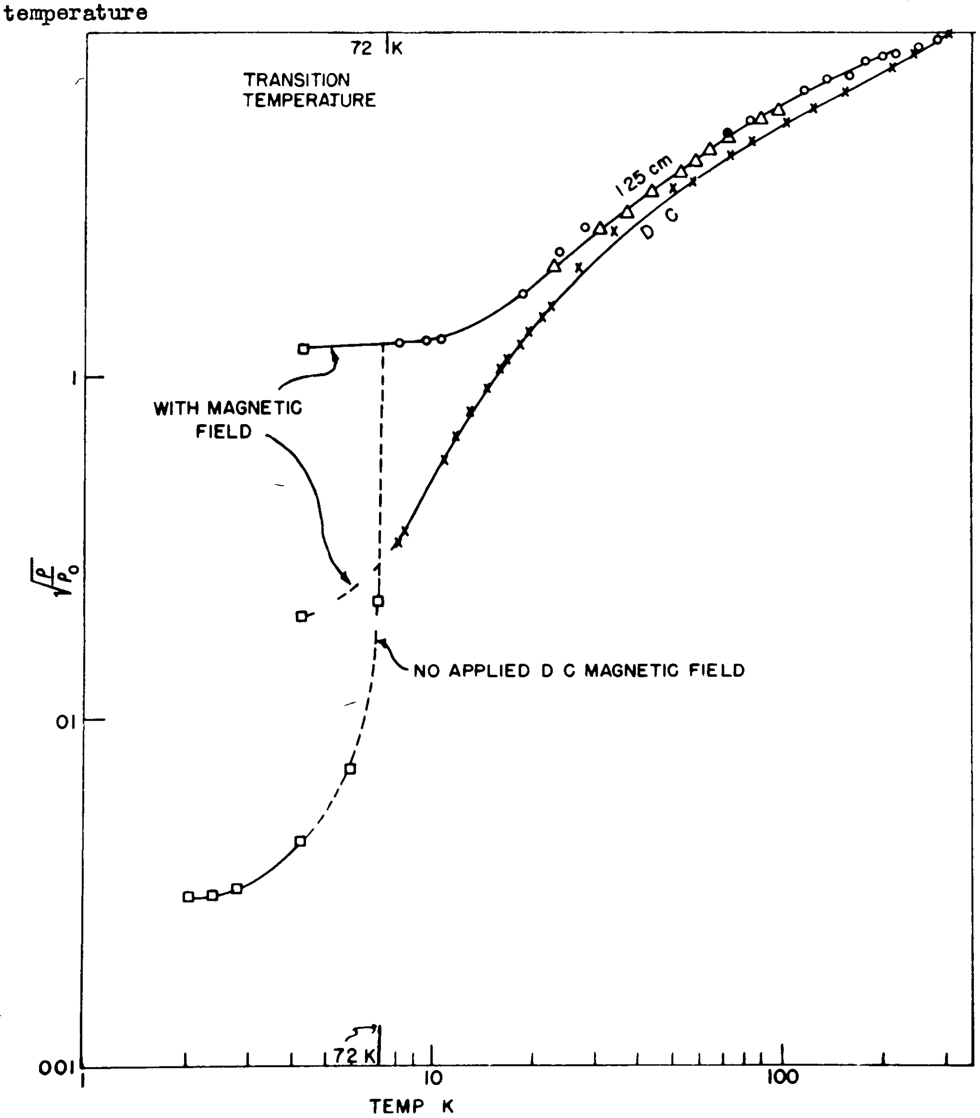

Figure 1

5 Magnetic Nuclear Resonance Experiments

Staff Professor F Bitter
N L Alpert
C G Lehr
S T Lin
H L Poss

Most of the effort during the present quarter has been devoted to analysis of resonance phenomena for finite rates of sweep through resonance, shop work on two magnets for experimental use during the coming year and preparation for another series of experiments using the cyclotron magnet Each of these items will be reported on separately below

Dynamics of Resonance Phenomena When a solid or liquid is placed in a constant magnetic field H_z, a magnetic moment M_o per unit volume is produced due to the alignment of the nuclear magnetic moments In the presence of an additional field H_1 rotating with angular velocity ω at right angles to H_z a component of the magnetic moment having the same frequency of rotation as H_1 is induced Bloch[1] has shown that the maximum value of this component when H_z and ω are constant or vary sufficiently slowly is

$$\frac{M_o}{2}\sqrt{\frac{T_2}{T_1}} \tag{1}$$

The resonance curves actually observed by various experimenters show periodic disturbances near resonance ($\gamma H_z = \omega$ γ = the gyromagnetic ratio for the nucleus under investigation) These disturbances have not been satisfactorily explained in detail but are undoubtedly associated with the finite rate of sweep through resonance

The ratio of the relaxation times T_2/T_1 is in many cases small compared with unity The question arises as to whether by sweeping through resonance sufficiently fast a signal produced by the full magnetization M_o may not be observed simply because resonance is passed before interaction processes have time to reduce the rotating magnetization to its equilibrium value (1) above These considerations led to the following analysis

Bloch's equations for the three components of magnetization u parallel to H_1, v perpendicular to both H_1 and H_z, m parallel to H_z are

$$\begin{aligned} \frac{du}{d\tau} + \beta u + \delta v &= 0 \\ \frac{dv}{d\tau} + \beta v - \delta u + m &= 0 \\ \frac{dm}{d\tau} + \alpha(m - M_o) - v &= 0 \end{aligned} \tag{2}$$

$$\tau = |\gamma| H_1 t, \quad \alpha = \frac{1}{|\gamma| H_1 T_1}, \quad \beta = \frac{1}{|\gamma| H_1 T_2}, \quad \delta = \frac{|\gamma| H_z - \omega}{|\gamma| H_1} .$$

1 Phys Rev 70, 460 (1946)

A considerable study of the general solutions of these equations was made, assuming δ constant The results are not of sufficient interest to warrant reproduction in detail Suffice it to say that if the magnetization has some arbitrary initial value the approach to equilibrium has the character of a damped oscillation The frequency and the damping constants will in general be functions of T_1 T_2 and δ

For finite rates of sweep, δ is taken as a linear function of the time

$$\delta = \frac{1}{H_1}\frac{dH_z}{dt}t = \frac{\tau}{c}$$

$$c = \frac{\gamma H_1^2}{dH_z/dt}$$

In the following, solutions of (2) were sought for the case $T_1 = T_2 = \infty$, or $\alpha = \beta = 0$ With the substitution $x = \tau/\sqrt{c}$ Eqs (2) reduce to

$$\begin{aligned} \frac{du}{dx} &= -xv \\ \frac{dv}{dx} &= xu - \sqrt{c}\,m \\ \frac{dm}{dx} &= \sqrt{c}\,v \end{aligned} \tag{3}$$

Separating variables by successive differentiation the following equation is obtained for v

$$\frac{d^3v}{dx^3} + (x^2 + c)\frac{dv}{dx} + 3xv = 0 \tag{4}$$

The general solutions of this equation may be found for $x^2 \gg c$ and the solutions for u and m then follow from the first and last equations in (3) The particular solution of interest is that for which equilibrium is established far from resonance ($u=0$ $v=0$, $m=M_0$ for $x=-\infty$) This solution is given below as a function of $z = x/\sqrt{\pi}$ since the functions in question are tabulated in Jahnke and Emde in this form The solutions are

$$u = B A_1 \qquad v = B A_2 \qquad m = \frac{\sqrt{c\pi}}{2} B A_3 + M_0$$

$$\begin{aligned} A_1 &= -\sin\frac{\pi z^2}{2}\left[\int_0^z \cos\frac{\pi y^2}{2}\,dy + \frac{1}{2}\right] + \frac{\cos\pi z^2}{2}\left[\int_0^z \sin\frac{\pi y^2}{2}\,dy + \frac{1}{2}\right] \\ A_2 &= \sin\frac{\pi z^2}{2}\left[\int_0^z \sin\frac{\pi y^2}{2}\,dy + \frac{1}{2}\right] + \cos\frac{\pi z^2}{2}\left[\int_0^z \sin\frac{\pi y^2}{2}\,dy + \frac{1}{2}\right] \\ A_3 &= \int_0^z \sin\frac{\pi y^2}{2}\,dy\left[\int_0^z \sin\frac{\pi y^2}{2}\,dy + 1\right] + \int_0^z \cos\frac{\pi y^2}{2}\,dy\left[\int_0^z \cos\frac{\pi^2 y^2}{2}\,dy + 1\right] \end{aligned} \tag{5}$$

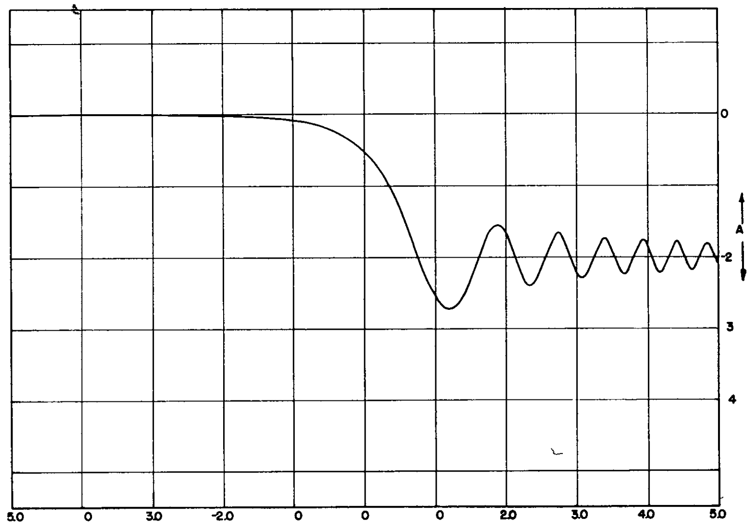

Figure 1.

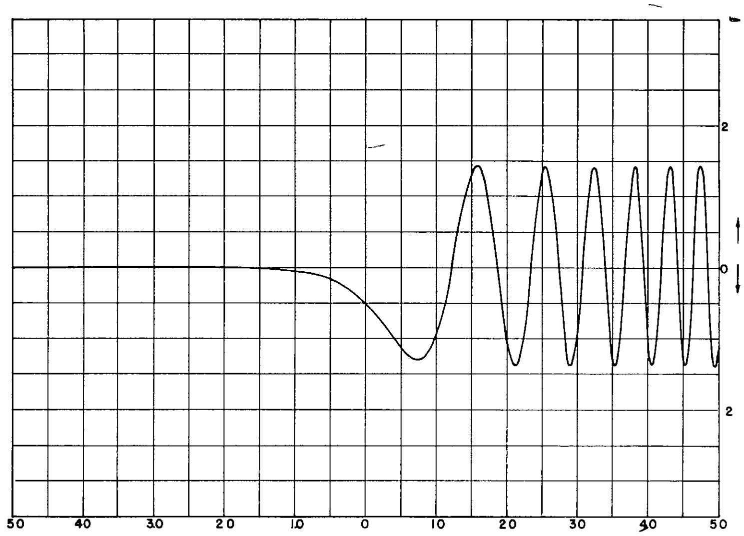

Figure 2.

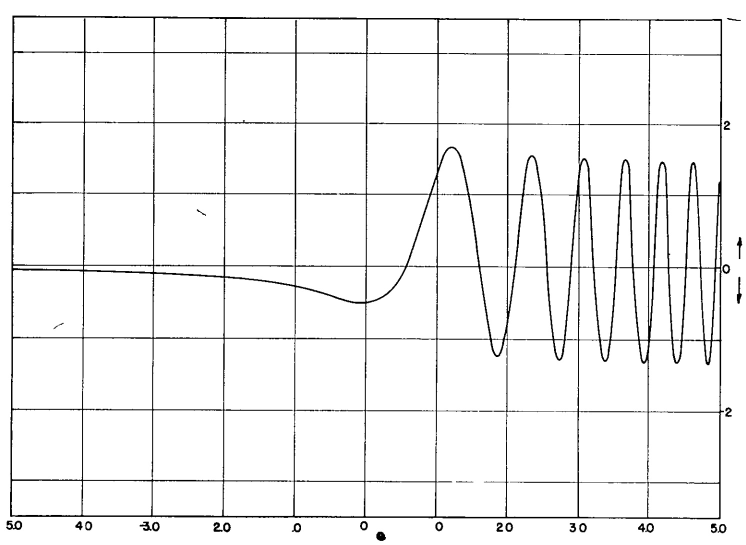

Figure 3.

The functions A_1 A_2 and A_3 are plotted in Figs 1 2, and 3 For $x^2 \gg c$, the condition

$$u^2 + v^2 + m^2 = M_o^2$$

is satisfied by choosing

$$B = -\sqrt{\pi c}\, M_o \qquad (6)$$

For sufficiently fast sweeps (small c) these solutions will hold approximately even through resonance at the origin but under these conditions the magnitude of the signals will be small because B is small

Solutions for a series of values of c from 0 1 to 10 were obtained from the M I T differential analyzer, using the above asymptotically valid forms (5) to establish initial conditions A few of these curves are reproduced in Figs 4-15

The results for $c > 1$ are not easy to compare with experiment Long before resonance is reached there are considerable oscillations which would be damped out to some extent in an actual experiment In this case of slow sweeps and large H_1 the damping terms will be important in determining the behavior at resonance Moreover to obtain these results the differential analyzer was pushed to the limit of its performance, and there is some question as to the correctness of some aspects of the curves, for example, the increasing amplitude of the oscillations for large positive values of x

It is interesting to note that for the limit of slow sweeps and large H_1, the equations of motion have at least one solution satisfying $u = v = 0$, $m = M_o$ far from resonance in addition to the well-known solution

$$u = \frac{M_o}{\sqrt{1+\delta^2}}, \quad v=0 \quad m = \frac{\delta M_o}{\sqrt{1+\delta^2}}$$

This is

$$\begin{aligned} u &= \left[-\frac{\delta}{1+\delta^2}\cos\sqrt{1+\delta^2}\,(\tau-\tau_o) + \frac{\delta}{1+\delta^2}\right] M_o \\ v &= \left[-\frac{1}{\sqrt{1+\delta^2}}\sin\sqrt{1+\delta^2}\,(\tau-\tau_o)\right] M_o \\ m &= \left[\frac{1}{1+\delta^2}\cos\sqrt{1+\delta^2}\,(\tau-\tau_o) + \frac{\delta^2}{\delta^2+1}\right] M_o \end{aligned} \qquad (7)$$

where τ_o is an arbitrary phase constant The character of these solutions is shown in Figs 16 17 and 18 For simplicity the oscillations are omitted The solid lines show the values around which the functions oscillate and the dotted lines show the limits of the oscillations The character of these results is similar to those obtained on the differential analyzer for c = 10 in that there are marked oscillations on both sides of resonance but the details in the two cases are still markedly different

For values of c of the order of 1 or less however the results are more reliable

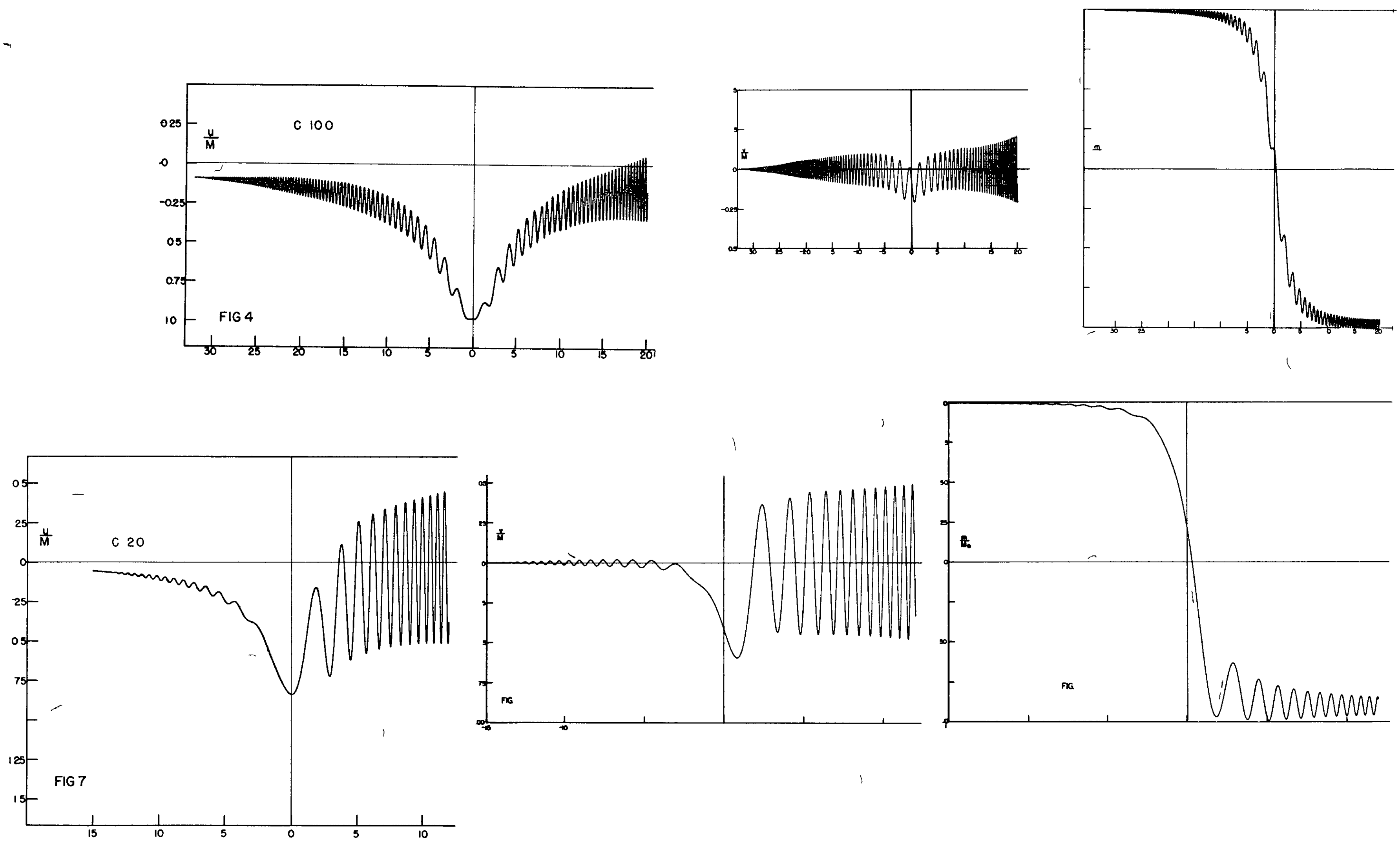

Figures 4 - 9 The three components of the nuclear magnetization u, v, m, plotted as functions of x for various values of the parameter c.

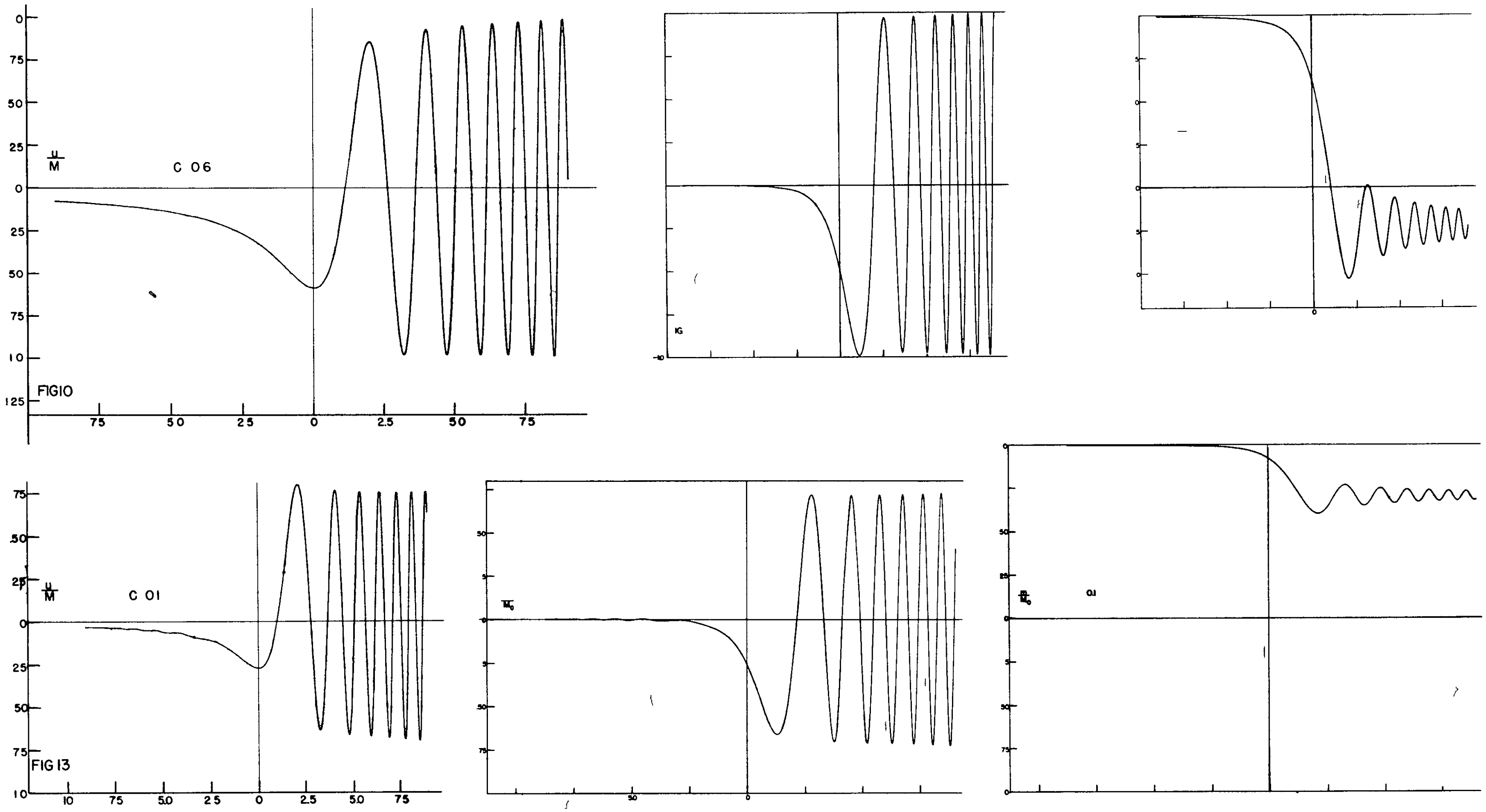

Figures 10 - 15. The three components of the nuclear magnetization u, v, m, plotted as functions of x for various values of the parameter c.

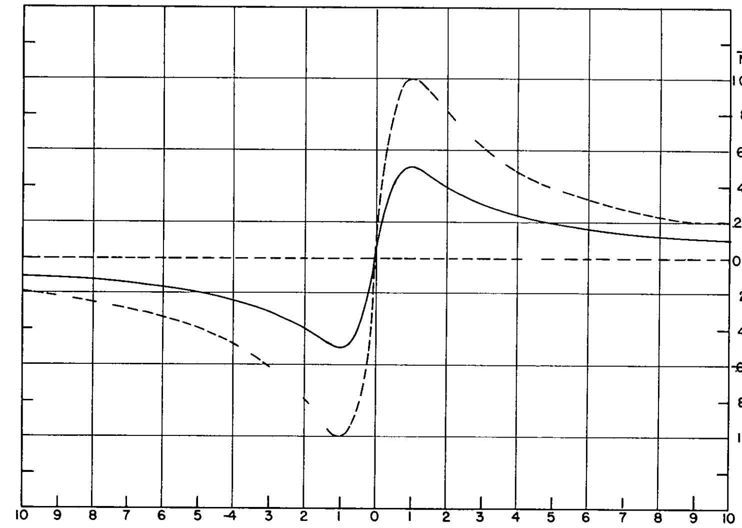

Figure 16.

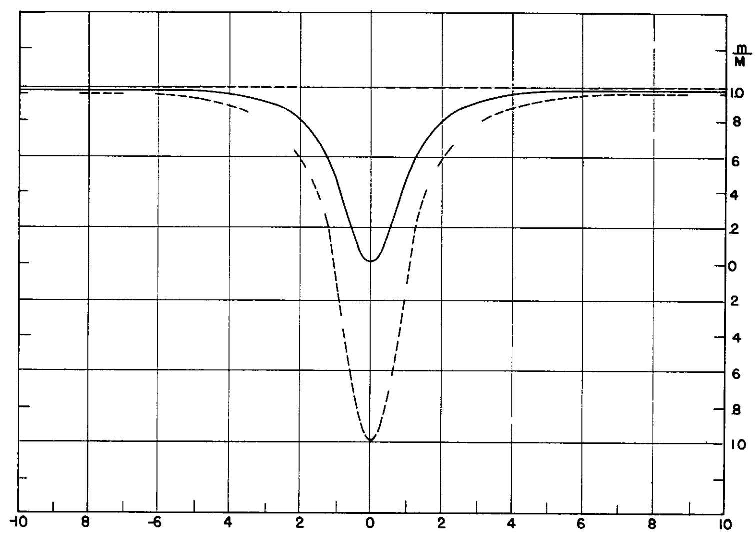

Figure 17.

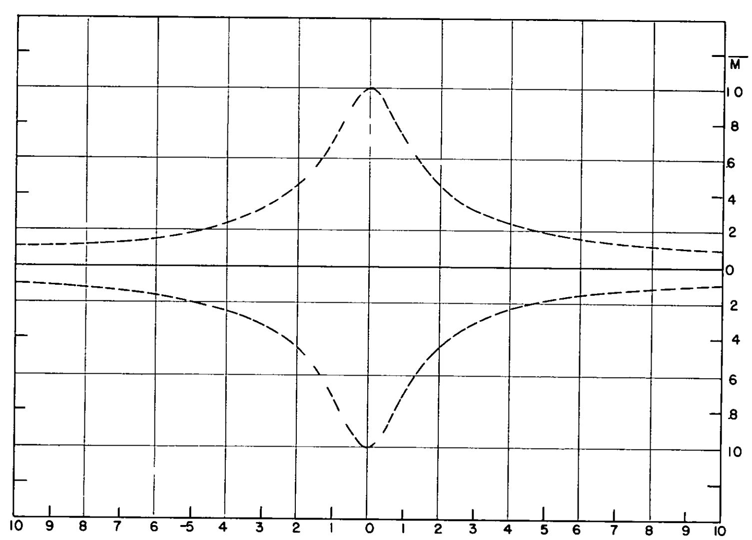

Figure 18.

and easier to interpret. Furthermore, they cover a range in which much of the experimental work has been done. (For protons, $H_1 \sim 0.1$ gauss or less, $dH_z/dt \sim 10^3$ gauss/second or greater). The appropriate time scale for each of the figures (4-15) may be found from the relation

$$x = \frac{1}{H_1} \frac{dH_z}{dt} t . \tag{8}$$

For sufficiently fast sweeps, the region of resonance can be traversed before the sample has time to demagnetize. Moreover, since c depends on H_1^2, it will in general be possible to choose H_1 and dH_z/dt in such a way that the maximum possible signal, corresponding to the full magnetization M_o, is obtained. In other words, it will be possible to choose H_1 and dH_z/dt in such a way that

$$\frac{1}{H_1} \frac{dH_z}{dt} T_2 \gg 1$$

and at the same time

$$c = \frac{\gamma H_1^2}{dH_z/dt} \sim 1 \quad . \tag{9}$$

In addition, in order to obtain large signals under these conditions, it is essential that equilibrium be established before resonance is approached. This may mean that a sinusoidal modulation field may be unsatisfactory. A circuit which makes it possible to wait off resonance for times sufficient to approach equilibrium, or of the order of T_1, and then sweep through resonance at a rate determined by (9), may eventually be desirable in experiments on small numbers of nuclei.

A detailed comparison with experiment is not possible at present. All that can be said is that for $c < 1$, the amplitude of the observed signal decreases, and that there is at least a qualitative similarity between such observed curves as that shown in Fig. 19, a proton resonance at 30.5 Mc, and the theoretical curves with superimposed damping.

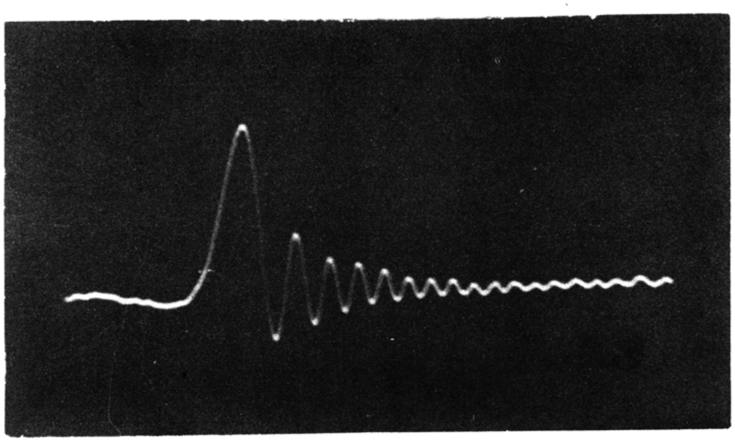

Figure 19.

Construction of Magnets for Future Use Reassembly of a solenoic having a 4-in inside diameter in which a field of 60,000 gauss can be produced is practically completed The 17-kw motor generator set is in operation It is planned to use this magnet for resonance experiments on solids as well as for adiabatic demagnetization experiments for which it was originally built

An iron-core magnet with 8-in diameter poles is also in the shop The iron parts are completed and material for winding the coils is at hand

Experiments now in Progress Experimental work now in progress falls into two classifications (1) a study of properties of solids and liquids, with particular reference to λ-point transitions in solids and rotational states in solids and liquids, and (2) determination and accurate measurement of nuclear g-factors

In reference to the λ-point transitions there are at present three theoretical mechanisms proposed to interpret these transitions, according to Professor L Tisza These are (a) a transition from hindered to free rotation of the molecules in the solid, (b) a transformation from an ordered to a disordered orientation, (c) a displacive transformation, in which the unit cell of the crystal undergoes a small distortion From previous results with methane, it is known that the first of these mechanisms can be easily identified, provided the rotations have frequencies much greater than the resonant frequency used (about 30 Mc) It is hoped that experiments now in progress on a variety of substances will reveal a correlation between the nuclear resonances and each of the mechanisms described above

As a preliminary to anticipated investigations of resonance phenomena involving nuclei with g-factors between 0 1 and 10 the design of apparatus which will enable us to use a wide range of resonant frequencies is being considered An investigation of Tl_{205} and Tl_{203} is in progress This makes use of the same circuits previously described Resonances have been observed in both isotopes Their magnetic moments are about 10 per cent higher than the value 1 45 nuclear magnetons found by spectroscopic means More accurate results will be given in the next report

6 Adiabatic Demagnetization

Staff Professor L Tisza
Dr J M Luttinger

The studies of dipole-dipole interaction (as discussed in previous progress reports) have been brought to a close These researches concerned themselves largely with the study of the behavior of completely (or almost completely) ordered arrays of paramagnetic ions in cubic crystals The calculations are confirmed in a general fashion by the measurements of de Haas and Wiersma Furthermore, suggestions have been made for experiments which would form a positive test of the theory The above-mentioned work formed the basis of a doctorate thesis[1]

---

1 J M Luttinger "Theory of Dipole Interaction in Paramagnetic Crystals," MIT 1947

II D 7 The Classification of Phase Transitions

Staff Professor L Tisza

The phase transitions connected with the so called λ-anomalies of the specific heat do not conform to the scheme of the Gibbs phase rule An extension of this scheme has been advanced by Ehrenfest who postulated the existence of higher order transitions Within this purely thermodynamic scheme no really satisfactory explanation of the frequent occurence of this phenomenon can be given A more specific classification is obtained by a method going somewhat beyond the scope of the purely phenomenological thermodynamics According to this generalized definition phases correspond to separate regions in Γ-phase space A phase transition is said to be of the first kind if the separation is realized in ordinary space, and of the second kind if it occurs in another subspace of phase space A system consisting of two phases of the first kind depends linearly on the amount of the phases present (surface effects may be neglected), hence the phase rule follows Examples for such transitions are condensation, freezing and the ordinary allotropic transformations, all of which are accompanied by latent heat (first-order transitions)

In case of the allotropic transformations two cases have to be distinguished (i) the symmetry groups of the phases are unrelated (neither is a subgroup of the other) (ii) the symmetry group of one phase is a subgroup of the other Only in case (i) is a latent heat present whereas case (ii) corresponds to gradual transitions with small anomalies of the specific heat (i) and (ii) correspond to transitions called reconstructive and displacive by Professor Buerger Examples for the latter are the α-β transition of quartz, Rochelle salt $BaTiO_3$ etc

In transitions of the second kind the phases are mixed, hence the phase rule is not valid and the transition is gradual Examples are superconductivity, liquid helium, ferromagnetism, order-disorder transformations rotational transitions etc The question of physical interest is to establish the nature of the phases which appear mixed Such a discussion has been carried through for the case of the hydrogen halides (See the April 15 Progress Report)

E PARAMAGNETISM AT MICROWAVE FREQUENCIES

Staff Dr C Kittel
Dr J M Luttinger

We have begun studies on the nature of the effects of magnetic and internal electric fields on the energy levels of paramagnetic ions placed in crystals For certain salts this effect (known as the crystalline Stark effect) can be expected to give level splittings in the neighborhood of 0 1 cm^{-1} Such salts will therefore have a microwave absorption spectrum and the study of this absorption would give information about the internal electric field of the crystal In the process of theoretical study are

(1) The splitting of a level in an electric field of given symmetry

(2) Selection rules for electric and magnetic dipole transitions between the different levels

(3) The effect of an external magnetic field on the split levels